strain
An International Journal for Experimental Mechanics

Fatigue on Shot-Peened Gears: Experimentation, Simulation and Sensitivity Analyses

G. Olmi, M. Comandini and A. Freddi

DIEM Department, Engineering Faculty, University of Bologna, Viale del Risorgimento, 2, 40136 Bologna, Italy

ABSTRACT: The present paper deals with fatigue experimentation and with the application and improvement of predictive models; in addition, a sensitive analysis is performed on the main factors related to the shot-peening treatment and on the efficiency of the aforementioned models. The research involved gears, made of high-strength steel and carburised, quenched, ground, shot-peened and superfinished. The experimental campaign initially dealt with the investigation into the influence of isotropic superfinishing; the attention was then focused on shot peening and how to optimise the fatigue limit, by a suitable choice of operative parameters. The option of duplex peening for further fatigue improvement was also considered. Results concerning component residual stress distributions and fatigue limits were then processed by investigating their sensitivity with respect to driving factors, namely the shot diameter and the Almen intensity. Two theories for fatigue prediction (the method of the relative stress gradient and the theory of critical distances) were reviewed for application to shot-peened components, with a comparison between experimental and numerical results. A comparative analysis was then performed on the two theories, on the basis of the number of data inputs, advantages and drawbacks, while sensitivity analyses focused on how uncertainties affecting input data propagate to predictive results.

KEY WORDS: *bending fatigue, gears, isotropic superfinishing, sensitivity analysis, shot peening*

Introduction

The failure of gears often occurs through a process of fatigue, which is usually attributed to both material properties and gear design together with working conditions. The improvement of the fatigue strength of gears is therefore of great importance in attaining increased load-carrying capacities and in improving the components and the reliability of the entire machine. As most bending fatigue failures initiate at or close to the surface, different types of thermo-mechanical, thermo-chemical and surface treatments are often applied to modify the material properties at the surface. These treatments have the basic feature of being carried out to harden the superficial layer, where initiation usually takes place [1–3].

It is well known [4] that residual stress distribution has a role in the improvement of component fatigue strength: based on this concept several treatments such as shot peening were developed. Such treatments lead to the generation of quite high-compressive residual stress on the surface and just beneath it. Shot peening is affected by several operative parameters that may significantly change the performance improvement. Several factors, such as the diameter of the outlet for peen shot, pressure and the impact angle, are usually accounted for in the Almen intensity. However, experimentations conducted in Ref. [5] confirmed that this parameter alone is not sufficient to fully describe residual stress distribution. For this reason, several authors [2, 3, 6] suggested the introduction of a second parameter, the peen diameter. In Ref. [2], the process of residual stress generation is widely investigated: it is mainly related to three events: surface stretching, flow beneath the surface due to the Hertzian pressure and transformation of the residual austenite into martensite in quenched components.

In Refs [2, 6], it is observed that the peening treatment mainly influences the position and the intensity of the sub-surface peak: in particular, the location of the peak depends on the size of the contact area, and consequently on the shot size (the larger the peen diameter, the deeper the peak), while the peak value is related to the impact energy transmitted to the target, which is proportional to the Almen intensity. However, the aforementioned trends are usually based on empirical observations without an analysis of significance and of nonlinearities. Moving on to the effect on bending fatigue,

doi: 10.1111/j.1475-1305.2009.00685.x

it was often noted that crack initiation takes place on a sub-surface layer on shot-peened parts [3, 7–11] and that the residual stress field tends to reduce the crack propagation rate, rather than to prevent nucleation [6, 9–12].

The increase in the fatigue limit is dependent on the operative parameters and on material resistance and toughness: 20% is a typical value for increment on medium-to-high-strength steels [3, 13]. In Ref. [3], a well-structured methodology, based on design of experiment (DOE), is widely and systematically applied for shot-peening parameter optimisation.

A further option for the peening treatment consists of the execution of an additional peening, to achieve a 'duplex peening' [1, 14]. The effect of duplex peening on the fatigue limit is quite controversial, due to poor experimentation in this field: some tests, reported in Ref. [1], showed an insignificant influence on both residual stress peak value and fatigue limit.

Another treatment, whose effect is still under investigation, is called isotropic superfinishing (ISF) [15]. A proprietary chemical compound is used in vibratory finishing bowls or tubes in conjunction with high-density, non-abrasive media, made of plastics or, more frequently of ceramics. The process takes place at ambient temperature: the chemical compound produces a stable, soft conversion coating on the treated surface. The rubbing motion due to vibration and to the media makes the conversion coating continually reformed and wiped off: at this stage of the treatment, surface levelling is produced, coating off the 'peaks' and leaving the 'valleys' untouched. This mechanism is continued in the vibratory machine until the surface is free of asperities. Finally, the chemical compound is rinsed off with a neutral soap, which completely wipes off the conversion coating: the treated surface assumes the typical mirror-like aspect. At the end of the process, a super smooth surface, with very low average roughness (0.025–0.050 μm), can be obtained. As a consequence, wear and friction are also strongly reduced, while very positive results concerning rolling/sliding contact fatigue are emphasised in Refs [15–17]: any pitting failure is minimised, or even eliminated on superfinished surfaces. In Ref. [15], it is remarked that the ISF treatment can lead to very positive results, if practiced after the shot-peening treatment: on the one hand, the residual stress distribution is not altered; on the other hand, lubrification properties are magnified by the ultra-smooth surface (due to ISF) with little indentations (due to shot peening), which are suitable for lubrificant retaining. Further research, described in Ref. [18], showed that the highly polished surface also has a positive effect on bending fatigue, even if reported experimentations involved only low- and medium-hardness steels. For high-hardness steels, little experimentation was conducted and just a few results are shown in Ref. [15].

Some simulative models were proposed for the prediction of the fatigue behaviour of shot-peened components [2, 6, 9]. In Ref. [2], a linear relationship was proposed between residual stress peak value and the fatigue limit; other models are reported in Refs [10, 19]. Some studies [20] aim at relating fatigue endurance to relative stress gradient (RSG): Eichlseder [21, 22] determines the fatigue limit as an interpolation between material experimental data sets, with the knowledge of the RSG, evaluated by FEM simulations. Finally, a novel approach on fatigue was proposed by Taylor in his 'theory of critical distances' (TCD) [23]. Both methods have often been applied for fatigue prediction but quite rarely on components containing high residual stresses, such as shot-peened ones. Moreover, no contributions have investigated the relationship between the two theories and provided a critical analysis also involving the robustness of the two methodologies with respect to input data uncertainties.

The present paper investigates several aspects related to fatigue improvement, focusing on the statistical significance of operative parameters, on the development of predictive models and on their comparison, based on sensitivity of results versus input data.

Materials and Methods

The component under study, Figure 1, is a spur gear, made from 16 NiCrMo 12 steel (chemical composition: C: 0.13–0.19%, Mn: 0.40–0.70%, Si: 0.15–0.40%, Cr: 0.80–1.10%, Ni: 2.70–3.20%, Mo: 0.30–0.40%, $S \leq 0.035\%$, $P \leq 0.035\%$). Each sample was commercially carburised (at approximately 870 °C) to give a case depth of approximately 1.0 mm. This treatment was followed by oil quenching at 860 °C and annealing at 150 °C. Further surface treatments were grinding and shot peening, according to the details mentioned below, with the treated layer ranging from approximately 50 to 150 μm, depending on operative parameters [1, 24–26]. The samples were finally superfinished, by a chemically accelerated vibratory finishing process with an active chemical compound (REM, Southington, CT, USA) in a vibratory bowl (by Rösler Metal Finishing, Battle Creek, MI, USA), in conjunction with high-density, non-abrasive ceramic media, at ambient temperature for 2.5 h [15]. The surface hardness

doi: 10.1111/j.1475-1305.2009.00685.x

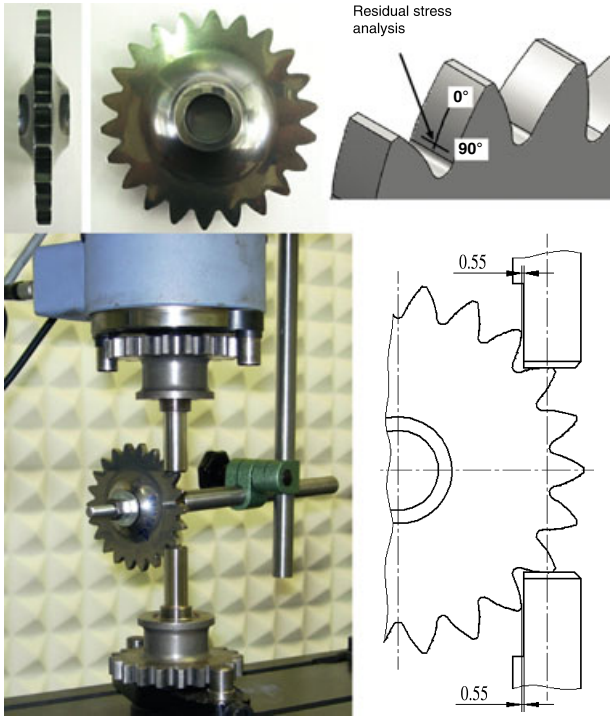

Figure 1: Gear component under test, location and directions for X-ray residual stress measurement and experimental set-up for fatigue tests

was measured at the end of the manufacturing process: after cutting a gear slice, a 730–750 HV hardness level was detected at the root of the tooth.

All gears (31) had the following features: 22 teeth, modulus 4 mm, face width 5.5 mm, addendum 3.73 mm, dedendum 5.29 mm with a correction factor of 0.96.

Experimental tests were carried out on a resonant testing machine (Rumul, Neuhausen am Rheinfall, Switzerland) with a loading device, designed for this particular application [27, 28], shown in Figure 1. Tooth bending fatigue tests were performed, by transmitting load through a pair of twin punches, along the machine vertical axis. Very strict geometrical and dimensional tolerances ensure a correct alignment and that just one tooth pair is subjected to load. The experimental tests were run according to the Dixon Staircase method [29] (applied also in Refs [3, 6, 9]).

Residual stresses after shot peening were measured by the X-ray diffraction method [2, 3, 6, 24, 30–32] and their values were estimated on the basis of the $\sin^2 \Psi$ method with Cr Kα radiation on the {211}-plane of the Fe (α) bcc (body-centred cubic) phase (XStress3000; Stresstech, Vaajakoski, Finland). The measurement of the residual stress distribution was performed at the root of the tooth. The in-depth measurements required step-by-step removal of thin material layers: this operation was performed by using an electro-polishing facility, in order to prevent considerable alteration of the pre-existent residual stress state [24]. This procedure was followed by X-ray measurements: XRD values were then corrected to account for the effect of the progressive material removal, by using the method described in Ref. [33]. With reference to a location at the root of the tooth, the residual stress distribution was determined along two directions, perpendicular and parallel to the gear axis (referred to as 0° and 90° in Figure 1). In accordance with Ref. [34], the residual stress distribution was presumed to be equibiaxial: for this reason mean stress values were considered for further processing.

The fatigue tests were conducted under pulsating load, with the adoption of a non-zero minimum load (load ratio $R \cong 0.1$), to ensure the correct positioning of the gear with respect to the loading device. Each test session was performed up to gear failure or to infinite life (test stopped after 10^7 cycles).

The fatigue limits were initially calculated as loads applied by the two punches [29]. These loads were then converted into local stresses at the root of the tooth. For this purpose, a FEM model was developed [28] to carefully estimate the peak of stress at the root, due to tooth bending, as a function of the force applied by the punches to the faces of the pair of teeth under test. One-eighth of the gear (a quarter cut along a plane perpendicular to the gear axis) was considered to be meshed by solid eight-node linear brick, a reduced integration, hourglass control elements and adequately constrained for a free rotation around its axis. The transmission of the load was achieved by a full simulation of a punch: the force was applied at the contact between the punch and the tooth face (Figure 2). For simplification purposes the punch was presumed to be rigid, according to its high axial stiffness, much greater (about five times) than the tooth bending stiffness. This approximation was applied also in agreement with other numerical studies (such as Ref. [2]), where just the applied force was simulated.

The experimental campaign was divided into two phases, focused on the influence of ISF practiced after shot peening on fatigue performance and then on shot peening improvement and optimisation, by a careful analysis of process parameter impact.

In order to address the first question, the influence of ISF, fatigue tests were performed on two different gear sets, consisting of two gears each. All the gears were subjected to the following treatments: case-hardening, quenching, grinding and shot peening. A quite ordinary treatment was applied, with a common setting of operative parameters: shot diameter was 0.28 mm (conventionally referred to as S110, 0.28 mm = 0.28/25.4 ≅ 0.0110 inches = 110×10^{-4}

doi: 10.1111/j.1475-1305.2009.00685.x

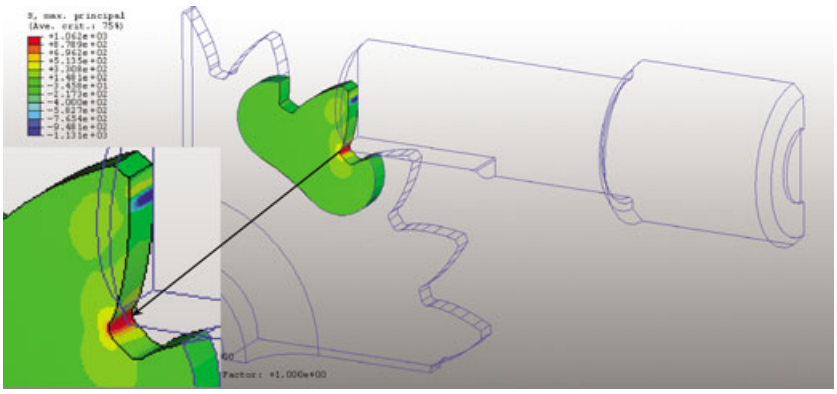

Figure 2: Finite-element method model to determine the stress at the root of the tooth, under a known force applied by the punches

Table 1: Two-factor plan of the investigated treatments

	Shot diameter			
Almen intensity	S110 (0.28 mm)	S170 (0.43 mm)	S230 (0.58 mm)	S330 (0.84 mm)
Low (10/12 A, pressure ≅ 4 bar)	•	•	•	•
Medium (14/16 A, pressure ≅ 4.5 bar)	•	•	• ♦	♦
High (18/20 A, pressure ≅ 5 bar)	–	–	♦	♦

inches, conventional general notation: S + shot diameter expressed in 10^{-4} inches) with 10/12 A Almen intensity (4 bar flow pressure). ISF treatment was then finally applied to one gear set: gears were finished by chemically accelerated vibratory finishing process, according to the procedure detailed above [15].

After studying the effects of ISF, attention was focused on the effects of shot peening, carried out with different operative settings, with reference to the shot diameter and the Almen intensity.

Eleven treatments were considered (all with ISF, with the same procedure, after shot peening) and arranged in the two-factor plan in Table 1, where the Almen intensity levels are equally spaced (low Almen 10/12A, medium Almen 14/16A, high Almen 18/20A, shot pressure varying from about 4 to 5 bar), while the shot diameter values are expressed in mm and in the conventional notation. The experimentation accounted for both single- and duplex-peening treatments. In particular, the symbol (•) denotes single peening, while the symbol (♦) indicates that an additional peening was performed with ceramic shots with a diameter of 0.15 mm (Z150, Z + shot diameter expressed in μm) at a pressure of 2 bar.

Experimental Results and Discussion

Fatigue tests for determining the impact of ISF were first performed on the previously mentioned two gear sets. The results for superfinished and non-superfinished gears were then compared, as shown in Table 2. Load values in the first column refer to the maximum force F_{max}, transmitted by the two punches, while the symbols used in the following columns refer to test results. In particular, the symbol (×) indicates that tooth bending failure took place at the current (first column) maximum loading setting, while the symbol (O) indicates that no failure occurred after 10^7 cycles, so that the test was stopped and the related tooth pair was regarded as run-out. The diagrams on the right show the same results with reference to trial local (at the root of the tooth) stress levels and to the determined local fatigue limits. Residual stresses were also measured (Table 3) and compared, in order to investigate distribution altering due to ISF practiced after shot peening.

According to Table 3, the residual stress distribution in the shot-peened and superfinished gear is slightly lower with respect to the non-superfinished component; peak values (often related to the fatigue limits [2]) are, however, quite close. Only the values along the 90° direction (see Figure 1) seem to have a slight difference (946 versus 1082 MPa), but this is within the usual uncertainty affecting such results, which is about 5–10% (results averaged over the two directions, 0° and 90°, are 990 and 1052 MPa, with 6% difference). An analysis of variance (ANOVA) [35] was applied in order to compare these results, and confirmed that the slight differences are not significant at the 5% significance level. Results of data processing are shown in Table 3, where SSB_C

doi: 10.1111/j.1475-1305.2009.00685.x

Table 2: Results of the fatigue tests on the shot-peened non-superfinished (A) and superfinished (B) gears

(A)

F_{max} (kN)	1	2	3	4	5	6	7	8
12.00							X	
11.75						O		X
11.50					O			
11.25				O				
11.00	X		O					
10.75		O						

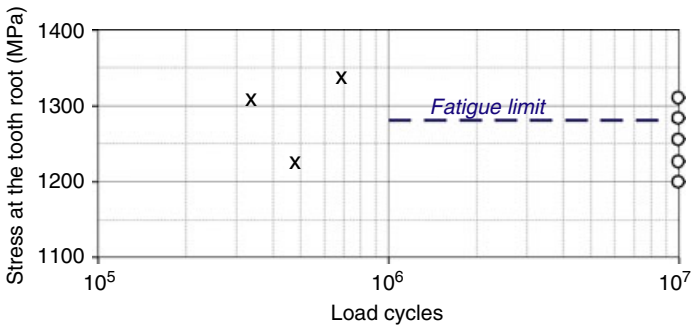

(B)

F_{max} (kN)	1	2	3	4	5	6
11.00	X		X			
10.75		O		X		O
10.50					O	

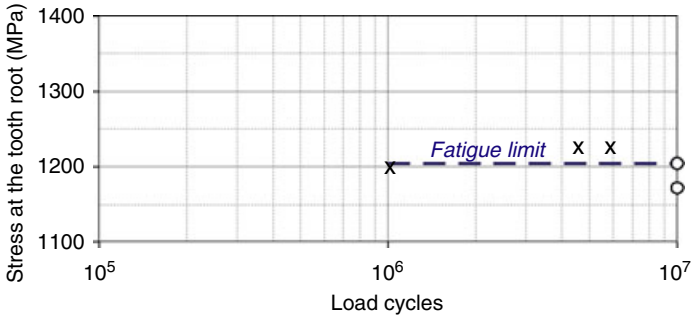

Table 3: Analysis of variance on residual stress peak values: comparison between superfinished and non-superfinished gears

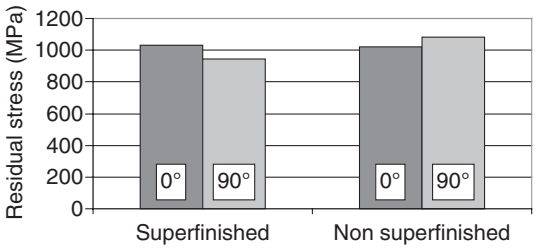

	SSQ	d.f.	MSQ	$F_{calc.}$	*P*-value
SSB_C	3906.25	1	3906.25	1.39	36 %
SSW_C	5612.5	2	2806.25		
Total	9518.75	3			

stands for sum of squares between columns (variance due to the impact of the ISF treatment on residual stress distribution), SSW_C stands for sum of squares within columns (variance due to experimental uncertainties), SSQ is a general term for sum of squares, d.f. stands for degrees of freedom, MSQ stands for mean squares, i.e. SSQ/(d.f.) and F_{calc} stands for *F* calculated (Fisher ratio). This result is also in good agreement with the conclusions of Winkelmann *et al.* [15], whose experiments suggested excluding any negative influence of ISF on residual stress field alteration.

The determination and comparison of the fatigue limits showed that they are very close too, with a difference of 6% (1203 versus 1280 MPa). According to Dixon and Massey [29] standard deviations

doi: 10.1111/j.1475-1305.2009.00685.x

were computed for the determined strengths, which were $s_1 = 21.0$ MPa for the peened superfinished component and $s_2 = 49.4$ MPa for the just peened one. As suggested also by failure and non-failure events in Table 2, the superfinishing treatment implies a strong reduction in data scattering, as confirmed by a high decrease in the standard deviation, reduced by 57%. The two fatigue limits were compared using an ANOVA [35] with error estimation as a quadratic average weighted on the number of degrees of freedom [3]. The test confirmed that no significant differences can be observed at the 5% significance level, i.e. results are statistically the same. Thus, ISF has a negligible effect on fatigue performance, but has a positive role in increasing result repeatability, as again confirmed by similar results in Ref. [15]. A possible explanation of this result is that the superfinishing treatment does not alter the residual stress distribution, which is mainly responsible for the averaged value of the fatigue limit but has a very positive role in making the surface conditions more homogeneous on the whole gear, which has an effect in reducing the small differences on surface properties among samples (tooth pairs subjected to tests), thus increasing repeatability.

The second stage of the experimental campaign was devoted to the study of the influence on fatigue of the main operative parameters in the peening process. The analysis dealt initially with residual stress distributions (Figure 3). In the case of single peening, the residual stress has a typical [1, 2, 9] distribution with a sub-surface peak at a depth ranging from 20 to 30 μm. Duplex peening is often applied with the aim of reducing surface roughness and making it more homogeneous, after peening treatments with high shot dimension and Almen intensity.

It can be noted that duplex peening leads to a significant increase in surface residual stress, while the typical trend has a plateau at the first sub-surface layers; however, the effect on the maximum residual stress value is very low, in agreement with Ref. [1]. ANOVA [35] was again used to analyse the effect of the two factors (shot diameter and Almen Intensity, for high-intensity duplex-peening treatments were considered) on the distribution shape (for a fixed impact density of 120%), particularly on peak value and depth. The response was that both factors have an influence on the peak value (at the 1% significance level), and that it is the Almen intensity which is the most significant, in agreement with Ref. [2]. The analysis was then refined, to investigate nonlinearity of the relationship between the Almen intensity and the peak value. For this purpose, the technique of

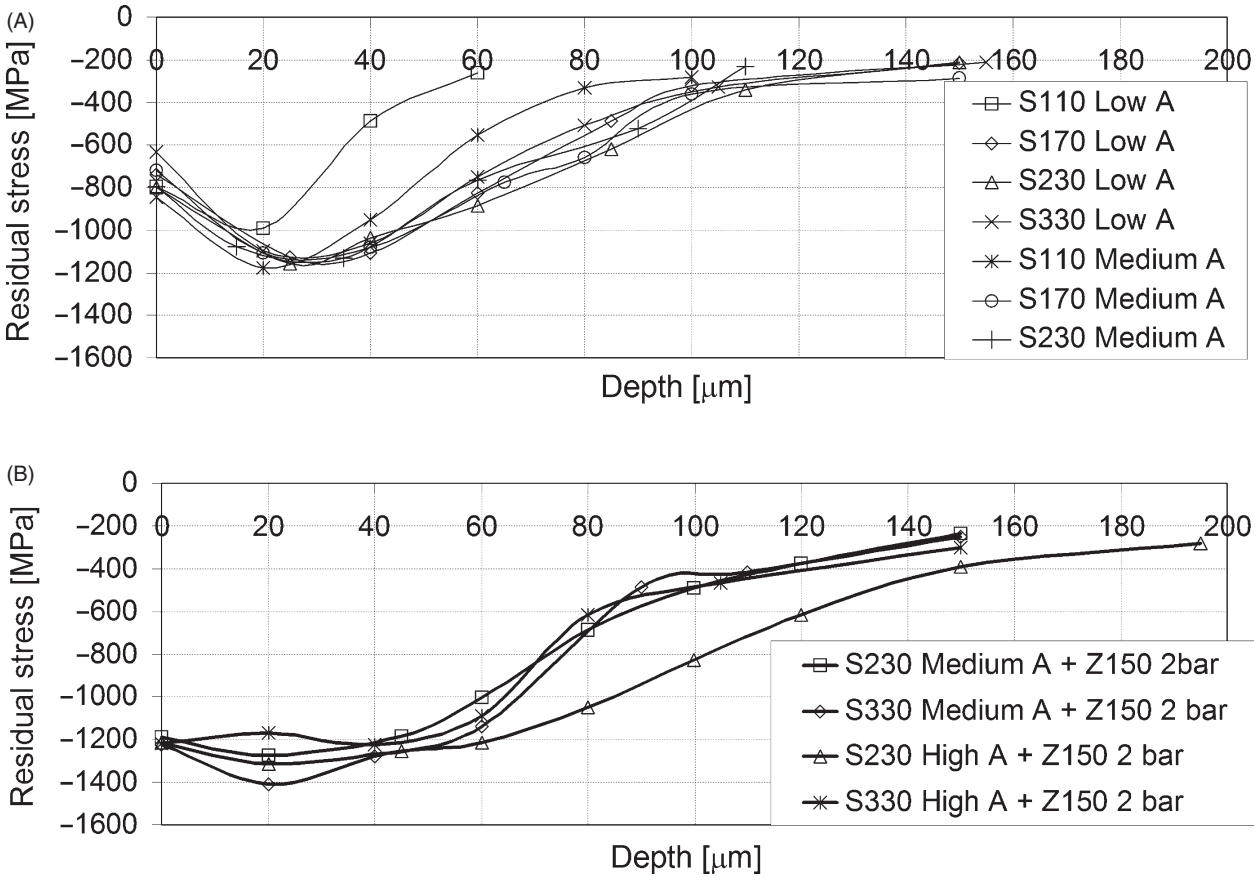

Figure 3: Residual stress distribution on single (A) and duplex (B) shot-peening treatments

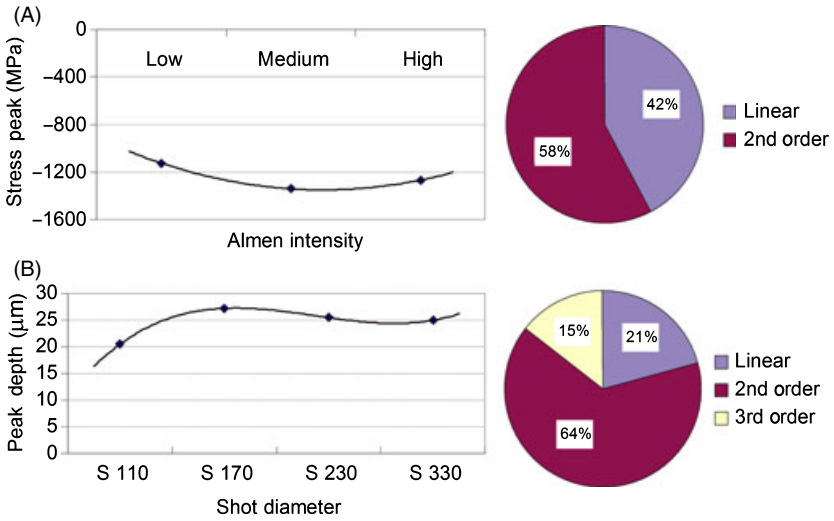

Figure 4: Linearity analysis on the dependences stress peak – Almen intensity (A) and peak depth – shot diameter (B)

the orthonormal decomposition of the sum of squares was applied [35]. Figure 4A shows the weight of linear and second-order terms in a pie diagram: they are both significant, but it is the nonlinear term which is the most effective. This result is confirmed also by the trend of the peak value with respect to the Almen intensity, shown on the left: the peak value initially increases as the intensity increases, until saturation is reached for high-intensity values: the peak value sensitivity to Almen intensity decreases as the intensity increases.

A similar analysis was performed on the peak depth (Figure 4B): it proved to be dependent on both factors, but the most significant factor was now the shot diameter, again in agreement with Ref. [2]. A nonlinearity analysis was thus performed with the same technique as before: the result was that the relationship between the shot diameter and the peak depth is highly nonlinear. The depth of the maximum residual stress has a high sensitivity to shot diameter at its lowest values, but this sensitivity is strongly reduced at the highest values.

Some shot-peening treatment combinations were excluded from the fatigue test planning; in particular, treatments with a high shot diameter and a low Almen intensity were rejected because they are difficult to perform, while treatments with very high Almen intensities were unable to meet requirements on surface roughness after the peening treatment. Moreover, the previous analysis showed that the improvements on the residual stress field at the highest values of the Almen intensity are very negligible, while the costs are significantly increased. The tests led to the following results, concerning the local fatigue limit at the root of the tooth (Figure 5) [27]. The histogram also reports the limits for non-shot-peened (and non-superfinished) gears and for the gears treated with S110 and low Almen intensity (10/12A, 4 bar flow pressure) and not superfinished. These results provided an opportunity to study the influence of duplex peening on fatigue. Figure 5 clearly shows that the determined limits are very close (1247 MPa for the treatment with S230 and medium Almen intensity and 1253 MPa in the case of duplex peening, just 0.5% increase). This response suggests that duplex peening has an insignificant influence on the fatigue limit, in agreement with Ref. [1]. By comparing the lists of failure and non-failure events (see Table 4, same symbols and notations as for Table 2) [27], it is clear that data scattering is highly reduced for the duplex-peened component. It implies that both standard error and standard deviation are much reduced by the additional peening treatment. From this point of view, duplex peening seems to

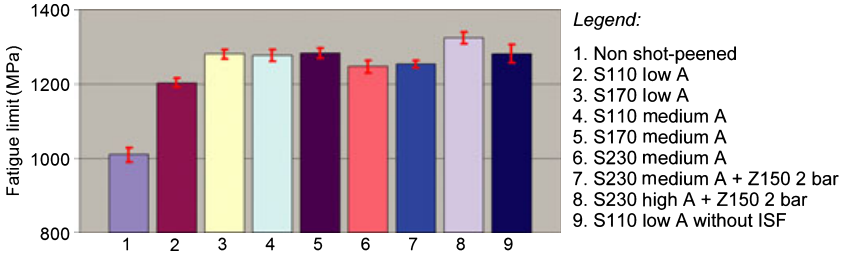

Figure 5: Local fatigue limits for the investigated treatments

doi: 10.1111/j.1475-1305.2009.00685.x

Table 4: Results of the fatigue tests on the gears with the shot-peening treatments S230 medium A (A) and S230 medium A + Z150 2 bar (B)

(A)

F_{max} (kN)	1	2	3	4	5	6	7	8	9	10
11.75							X			
11.50						O		X		
11.25	X				O				X	
11.00		X		O						X
10.7 5			O							

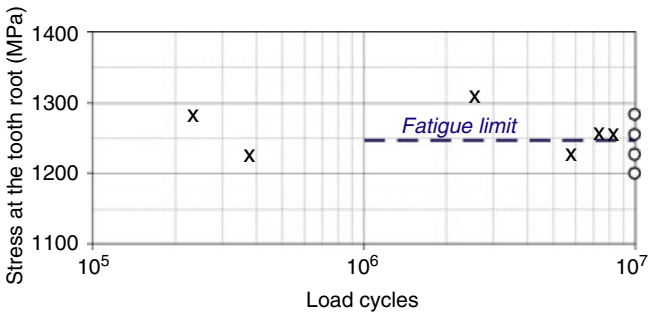

(B)

F_{max} (kN)	1	2	3	4	5	6	7	8	9
11.50	X						X		X
11.25		X		X		O		O	
11.00			O		O				

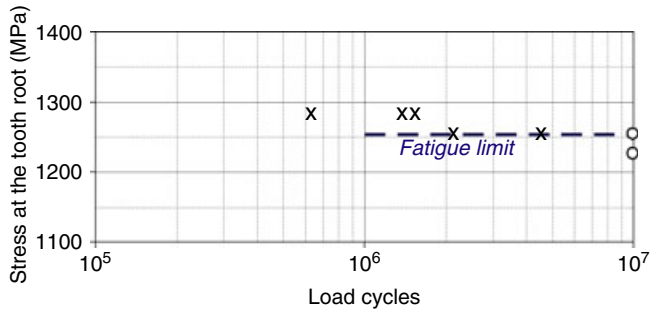

have an effect very similar to that of ISF on high-strength steels; the fatigue strength is left unchanged, but the standard deviation is decreased by 40%.

The results summarised in Figure 5 show that, depending on operative parameter choice, a fatigue limit increase from 19% to 31% can be obtained. This range of variation compares well with results reported in Refs [2, 3, 13, 31]. These results were also processed by an ANOVA (Table 5), with error calculation as degree of freedom-weighted average of

Table 5: Analysis of variance on the fatigue limits of the investigated treatments and orthonormal decomposition of the sum of squares

	SSQ	d.f.	MSQ	*F*calc.	*P*-v. (%)
Almen Int.	4485	2	2242	2.88	6.73
Shot diameter	2764	2	1382	1.77	18.20
Interaction	696	1	696	0.89	35.00
Error		42	Estimated: 779		
Total	7944	47			

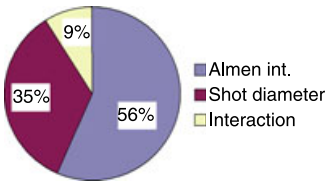

doi: 10.1111/j.1475-1305.2009.00685.x

variances according to Refs [3, 29, 35]. The analysis showed that Almen intensity and shot diameter are significant at the 7% and 18% significance levels respectively. The highest significance of the Almen intensity seems to confirm the common idea that the potentiality of the peening treatment is proportional to the Almen intensity value [6, 36]. This response also provides an explanation to what was observed in Ref. [2], concerning a linear relationship between the fatigue limit and the value of residual stress peak, previously proved to be related to the Almen intensity. However, the pie diagram in Table 5 shows that also the shot diameter has an impact: it contributes by 35% to the whole variance. This is in agreement with the observation [5] that the residual stress distribution cannot be completely explained by just considering the Almen intensity. The shot diameter also has a slight influence on residual stress distribution and consequently on the fatigue response. A brief comment should be made regarding the entities of the *P*-values of the effects related to the two factors: they are both higher than 5%, while in previous analyses (on residual stress distributions) they had been much lower. This means that, while the shot diameter and the Almen intensity have a great influence on the residual stress profile, they have an undoubtedly not unimportant, but lower influence on the fatigue limit. On high-strength steels the sensitivity of fatigue strength is much lower than the sensitivity of residual stress distribution.

Fatigue predictive models

One of the most recent models (by Eichlseder [21, 22]) for the simulation of component fatigue performance proposes that the local fatigue limit σ_f at a particular location of a component is characterised by an interpolation of fatigue limit in bending (σ_{bf}) and in uniform stress loading conditions (σ_{tf}). These data are evaluated by running experimental tests on un-notched specimens (with diameter b) made of the same material (constant K_D related to material properties). Equation (1) (Figure 6) gives the fatigue limit as a function of the RSG for the stress ratio R equal to −1. The RSG χ' can be computed according to Equation (2).

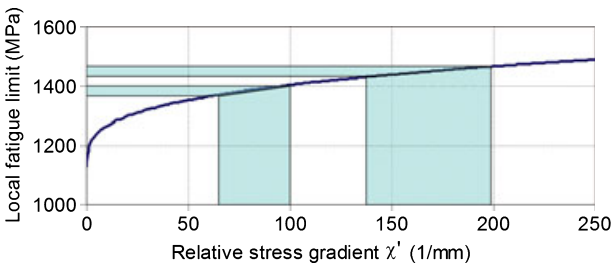

Figure 6: Nonlinear relationship between the predicted fatigue limit and the relative stress gradient

$$\sigma_f = \sigma_{tf}\left[1 + \left(\frac{\sigma_{bf}}{\sigma_{tf}} - 1\right)\left(\frac{\chi'}{(2/b)}\right)^{K_D}\right] \quad (1)$$

$$\chi' = \left(\frac{1}{\sigma_{max}}\right)\left(\frac{d\sigma}{dx}\right) \quad (2)$$

For different values of R, the calculated limit must be adjusted, considering the actual mean stress of the cycle, for instance, by constructing the Haigh diagram (Goodman linear model).

The RSG model was generalised here to the case of shot-peened components. This model was then used for fatigue limit prediction with reference to all the cases investigated in the present paper. The first step consisted of the determination of the total stress distribution at the root of the tooth, as a sum of the stress due to the external load, at its maximum value (by the FEM structural analysis) and the residual stress due to shot peening (Figure 3). Then, by applying Equation (2), the RSG was calculated at the surface layer for all the peening treatments. Thus, by substituting the so-determined RSG value in Equation (1), the local fatigue limit was calculated for any case. It must be remarked that the proposed methodology accounts for the residual stress field at two processing phases: to determine the total stress field (Figure 7A) and consequently to estimate the RSG, and then to finally adjust the final result as a function of actual mean stress [32, 34, 37, 38].

The results (limits for maximum stress) are shown in the histogram in Figure 7B, comparing experimental data to numerical predictions. The model was also applied to the case of non-shot-peened gear, considering the residual stress field due to the thermo-mechanical treatments. As can be noted in Figure 7B, the errors appear to be acceptable: the mean error is 4%, while the maximum one is 11%, for treatment 1, unpeened state, and for treatment 8, S230 High A, duplex peening. Some comments arise from these results: by observing the aforementioned histogram, it can be noted that for cases 1 and 8 the estimated limits are very close (1130 and 1170 MPa respectively), while the experimental results are quite different (1010 and 1320 MPa). For the unpeened component the result of experimentation is a little lower than expected: this difference could be due to the absence of surface treatments on the unpeened gears, having a roughness average about 10 times

doi: 10.1111/j.1475-1305.2009.00685.x

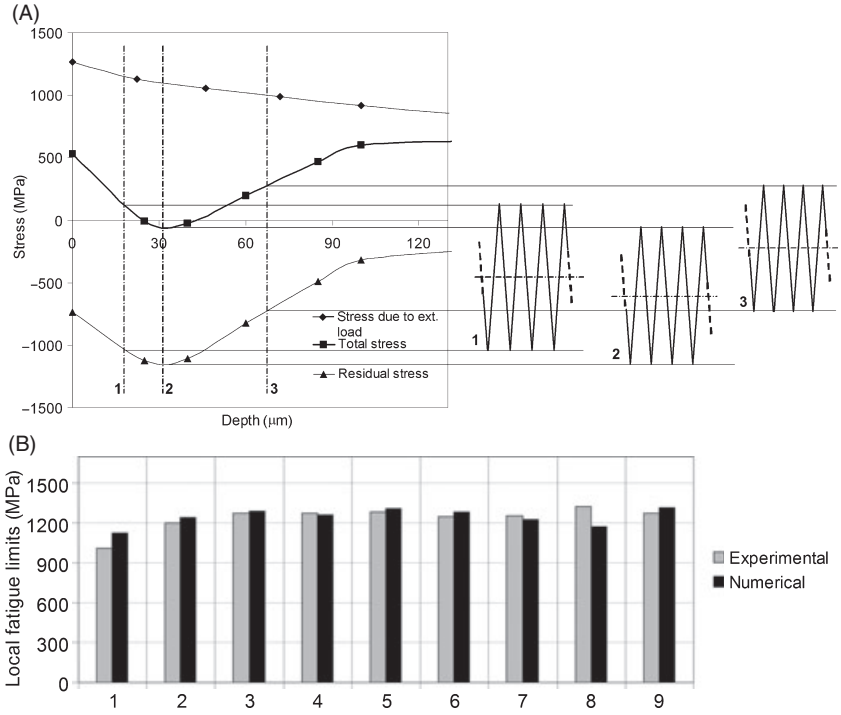

Figure 7: Determination of the total stress distribution (A) and comparison between numerical fatigue limit predictions and experimental results according to the relative stress gradient methodology (B)

greater than that of shot-peened superfinished gears, which implies a worse fatigue performance. As far as case 8 is concerned, it must be argued that in this case the residual stress distribution determines a high value of the RSG, about 117 mm^{-1}, according to Equation (2). Thus, by introducing this value in Equation (1), a quite high value of σ_f is obtained (1416 MPa) for $R = -1$. The classical Goodman linear model was then applied, to adjust this limit with reference to the current value of the mean stress, −550 MPa. Such a low value of the mean stress led to the underestimation of the fatigue limit described above. However, such a result does not appear to be due to a weakness of the model proposed by Eichlseder, but to the fact that the Goodman model is not specifically developed for fatigue limit estimation in the case of compressive mean stress and for cycles mainly in compression, for which the fatigue propagation is much slower. A similar result is observed in Ref. [32], where the conventional Goodman linear model is initially used to account for the residual stresses due to shot peening and to deep surface rolling. This procedure leads to an underestimation of the amplitude fatigue limits, being much lower than experimental yields.

A common drawback of the predicting models based on RGS estimation is that, if the stress distribution is very steep, it is often difficult to determine the actual gradient value. It would require the adoption of a finite-element model with a very high refinement, with long computational times and high costs. Consequently, it is essential that an underestimation on the gradient value does not imply too high an error on fatigue limit prediction. Moreover, the fatigue resistance is likely to have a saturation for high gradient values and not to increase indefinitely as the gradient increases. The RSG model by Eichlseder is not linear and its trend is similar to that of a logarithmic curve (the term K_D in Equation 1 can be assumed to be 0.3 for alloyed steel materials [22]): for this reason it has a good robustness (Figure 6) for huge values of the RSG (due, for example, to a shot-peening treatment). In the proposed cases, if RSG estimates had been affected by a 30% error, the aforementioned fatigue predictions would have been affected by just 1–3% errors.

In the last stage of the research the validity of another model, proposed by Taylor in his TCD [23], was the subject of further investigations. This is based on the concept that fatigue failure takes place when local stress variation at a 'critical distance' from the notch increases up to a 'critical value' (related to the fatigue limit of an un-notched specimen of the same material). This is called the point method (PM); otherwise the line method (LM) refers to a stress range averaged over a line, having a length related to the 'critical distance'.

Trying to compare the TCD with theories based on RSG estimation, the following remarks may be made. Both methods require finite-element analysis of stress

doi: 10.1111/j.1475-1305.2009.00685.x

distribution and some data of material characterisation. The RSG theory requires three parameters for describing the whole curve in Figure 6: two fatigue limits in two different loading conditions and the constant K_D. The TCD requires just two: a fatigue limit and the term ΔK_{th} (threshold value of the stress intensity factor range). In both cases the fatigue prediction is strictly dependent on one variable, the RSG and the stress field at the critical distance (TCD). Moreover, both methodologies are based on the concept that fatigue failure cannot be regarded as a punctual event: it is not the single peak of stress that implies crack initiation and propagation but the stress distribution around the concentration point. For the TCD (PM) it is more exactly the stress value at a certain point, but connected to the whole stress distribution.

Drawbacks may undoubtedly arise in the application of both models. The RSG may be difficult to compute, even if the proposed relationship to fatigue limit seems to be robust. On the other hand, the term ΔK_{th} could be difficult to determine, making it hard to correctly estimate the critical distance.

As a matter of fact, the present problem was remarkably complicated due to the surface thermo-mechanical treatments, responsible for the change in the material structure and for the generation of a high residual stress field. The RSG method needs the characterisation of the material in the same treatment condition (two fatigue experimental data sets and the constant K_D). On the other hand, the TCD needs the ΔK_{th} for a specimen in the current treatment condition. Moreover, in the authors' opinion, the role of mean stress for this method must be treated by running an iteration.

ΔK_{th} was initially assumed to be 12 MPa $m^{0.5}$ according to Taylor [23]. It must be observed that this input is determined for $R = -1$: for different loading cycles ΔK_{th} may be different, even if Taylor [23] remarks that the proposed method is robust on a wide range of variation for R.

The critical distance L was calculated, according to the following equation (PM):

$$L = \frac{1}{\pi}\left(\frac{\Delta K_{th}}{\Delta \sigma_0}\right)^2 \quad (3)$$

The term $\Delta \sigma_0$ denotes the fatigue limit of the material, equal to 1175 MPa, determined by running tests on un-notched specimens. In addition, this limit refers to the same loading condition with $R = -1$, which ensures the compatibility of terms ΔK_{th} and $\Delta \sigma_0$ introduced in Equation (3). For the aforementioned numerical values the result of Equation (3) is $L = 33$ μm: this distance is indeed very short and the related location surely lies within the thermo-mechanical treated layer. If supposing a pulsating load transmitted to the gear ($R = 0$), the stress at any tooth location ranges (Figure 7A) from the local value of residual stress (for null external load) to the local value of total stress (for maximum external load). Consequently, depending on the point, the material is subjected to a different stress cycle: for example, in Figure 7A three different cycles are shown, with reference to three different distances from the surface (lower, equal to and greater than the distance from the surface of the residual stress peak). The PM prediction is made by introducing in Equation (3) known values of $\Delta \sigma_0$ and of ΔK_{th} of this material, determined for the proper value of R, i.e. they depend on the mean stress. However, the mean stress is also dependent on the distance of the critical point from the boundary. This is a typical recursive problem that needs an iterative methodology in order to be solved. The stress range and the related mean stress are thus determined at the critical distance, initially computed for $R = -1$. A new value of the fatigue limit is then calculated for the new R value, estimated for the local mean stress.

By applying Equation (3) again, a new value of L is calculated and the procedure is continued for the following steps until a convergence is achieved. This procedure was applied to all peened components; moreover, as in the application of the RSG theory, the unpeened state was also considered, referring to the residual stress distribution, due to thermo-mechanical treatments. Procedure application required plotting stress–distance diagrams, like that in Figure 7A: for all the peened/unpeened states the iteration led to convergence, and final values for the critical distances and fatigue limits $\Delta \sigma_0$ (i.e. critical values) were computed. With reference to the peening treatments, it is interesting that all critical distances are very close to the distances of the residual stress peaks, i.e. the residual stress peaks are very close to the residual stress values at the critical distance, Figure 8A. The proper determination of the threshold ΔK_{th} for the current material and stress ratio could be a drawback in the application of the TCD. Poor data are often available in literature: for this reason, a sensitivity analysis was performed to investigate how uncertainties on the real value of ΔK_{th} may propagate to results of fatigue prediction. According to Taylor [23], two possible values for the threshold were considered, the aforementioned 12 and 9 MPa $m^{0.5}$: this range appears to be in agreement with the typical scattering for alloyed high-strength steels, for a stress ratio R lower than −0.5 (local stress cycle partially, sometimes mainly, in compression). The replication

doi: 10.1111/j.1475-1305.2009.00685.x

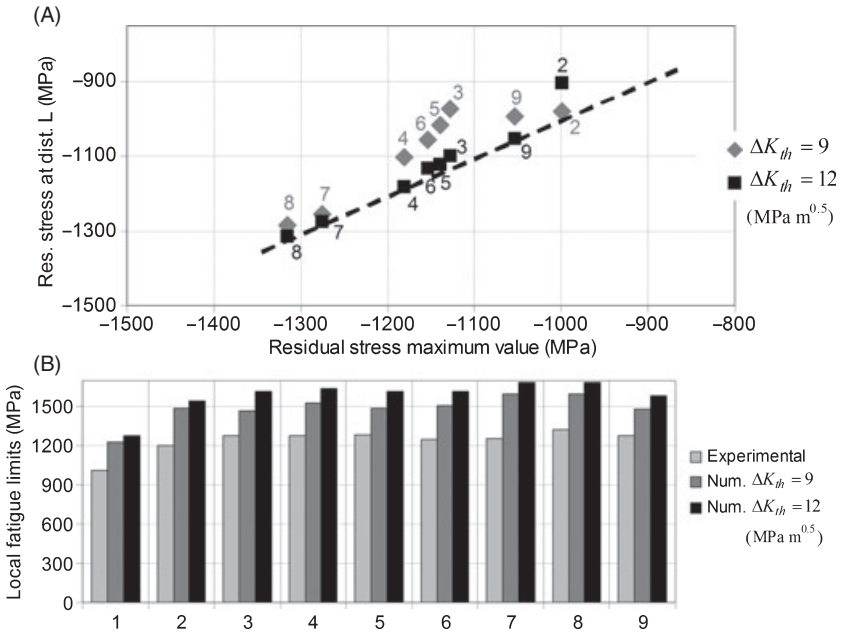

Figure 8: Residual stress at the critical distance L versus residual stress peak value (A) and comparison between numerical fatigue limit predictions and experimental results according to the theory of critical distances (B)

of the same procedure for ΔK_{th} = 9 MPa m$^{0.5}$ confirms a similar behaviour as for ΔK_{th} = 12 MPa m$^{0.5}$. The TCD, although not explicitly developed for shot-peened components, takes into account the influence of residual stress on the fatigue improvement. The higher the maximum value of residual stress, the lower the mean stress at the critical distance, and consequently the higher is the critical value. Moreover, the deeper the peak, the lower is the stress range at the critical distance.

The TCD procedure was then applied for fatigue limit determination: the loads at the fatigue limit were scaled in the ratio between the critical value $\Delta\sigma_0$ and the stress range at the critical distance. The results are shown in Figure 8B, where a comparison is made between experimental results and predictive results for ΔK_{th} = 9 and 12 MPa m$^{0.5}$, also testing model robustness. Despite a not completely satisfactory agreement with experimental results (errors range 20–30%), these results do not seem to be too greatly affected by the value of ΔK_{th} (Figures 8A and B). This is a confirmation of Taylor's remarks, regarding the robustness of the proposed model that supports its possible application with iterative determination of the critical distance and of the critical value in the case of the complex stress distribution due to a residual stress state.

Conclusions

Experimental results

- Isotropic superfinishing and duplex peening seem to have a similar role on fatigue performance: the fatigue limit is not influenced, but the standard deviation affecting results is considerably lowered.
- The ANOVA test showed that the peak of residual stress is mainly dependent on the Almen intensity, while the peak depth mainly depends on the shot diameter. Both relationships are nonlinear, with a saturation for the high values of the two parameters.
- The fatigue limit can be increased from about 20% to 30% with a suitable choice of operative parameters. ANOVA was again applied to test the sensitivity of the fatigue endurance to the two parameters of Almen intensity and shot diameter. The fatigue limit is mainly sensitive to the Almen intensity variations, but this sensitivity is much weaker than that of residual stress distribution.

Predictive models

- A comparative analysis was carried out utilising two criteria for fatigue failure prediction, the RSG method and the TCD in the non-common case of thermo-mechanical treatment of the component surface.
- The RSG requires three material parameters. They must be obtained by simple specimen tests but with the same condition of chemical composition and thermo-mechanical treatment. This may represent considerable difficulty.

doi: 10.1111/j.1475-1305.2009.00685.x

- The TCD requires only two material parameters, obtained by simple specimen tests in the same metallurgical state of the component. In this case too, the proper choice of ΔK_{th} can be a handicap, which is not easily overcome. In this case, an iterative methodology was proposed for the proper determination of the critical distance and of the critical stress, taking into account the distribution of residual stress. One interesting discovery was the strong correspondence between the distance of the critical point and the depth of the residual stress peak.
- For all the previous reasons, a sensitivity analysis was carried out to test the robustness of both models. The RSG model was tested with respect to uncertainties on the RSG distribution, while TCD was tested against the uncertainty of ΔK_{th} estimation. Both models appear relatively robust. RSG, which agrees with experimental results with an error not exceeding 11% (average value of 4%), denotes a weak propagation of the error affecting the RSG to the final prediction of the local fatigue limit. The TCD displays a lower agreement (errors range 20–30%) with the experimental results, but the scatter of the predicted results is small with respect to ΔK_{th} variations.

REFERENCES

1. Shaw, B. A., Aylott, C., O'Hara, P. and Brimble, K. (2003) The role of residual stress on the fatigue strength of high performance gearing. *Int. J. Fatigue* **25**, 1279–1283.
2. Benedetti, M., Fontanari, V., Höhn, B.-R., Oster, P. and Tobie, T. (2002) Influence of shot peening on bending tooth fatigue limit of case hardened gears. *Int. J. Fatigue* **24**, 1127–1136.
3. Croccolo, D., Cristofolini, L., Bandini, M. and Freddi, A. (2002) Fatigue strength of shot peened nitrided steel: optimization of process parameters by means of design of experiment. *Fatigue Fract. Eng. Mater. Struct.* **25**, 695–707.
4. Mann, J. Y. (1967) *Fatigue of Materials—An Introductory Text*. Melbourne University Press, Melbourne.
5. Herzog, R., Zinn, W., Sholtes, B. and Wohlfahrt, H. (1996) The significance of Almen intensity for the generation of shot peening residual stresses. *Proc. VI Int. Conf. on Shot-Peening*, 270–281.
6. Guagliano, M. and Vergani, L. (2004) An approach for prediction of fatigue strength of shot peened components. *Eng. Fract. Mech.* **71**, 501–512.
7. Wang, S., Li, Y., Yao, M. and Wang, R. (1998) Fatigue limits of shot-peened metals. *J. Mater. Process. Technol.* **73**, 57–63.
8. Jiang, X. P., Man, C. S., Shepard, M. J. and Zhai, T. (2007) Effects of shot-peening and re-shot-peening on four-point bend fatigue behaviour of Ti–6Al–4V. *Mater. Sci. Eng. A* **468–470**, 137–143.
9. Colombo, C., Guagliano, M. and Vergani, L. (2005) Pallinatura di acciai nitrurati: analisi sperimentale e numerica. *Proc. XXXIV Convegno Nazionale AIAS*, Milano.
10. Fathallah, R., Laamouri, A., Sidhom, H. and Braham, C. (2005) High cycle fatigue behavior prediction of shot-peened parts. *Int. J. Fatigue* **26**, 1053–1067.
11. Wagner, L. (1999) Mechanical surface treatments on titanium, aluminium and magnesium alloys. *Mater. Sci. Eng. A* **263**, 210–216.
12. Song, P. S. and Wen, C. C. (1999) Crack closure and crack growth behavior in shot peened fatigued specimen. *Eng. Fract. Mech.* **63**, 295–304.
13. Ohsawa, M. and Yonemura, T. (1984) Improvement of hardened surface by shot peening. *Proc. II International Conference on Shot Peening (ICSP2)*, Chicago (USA), 147–158.
14. Benedetti, M., Azanza Ricardo, C. L., Santus, C. and Fontanari, V. (2007) Studio dell'effetto della pallinatura sul comportamento a fatica della lega Al-7075-T651. *Proc. XXXVI Convegno Nazionale AIAS*, Napoli.
15. Winkelmann, L., Michaud, M., Sroka, G. and Swiglo, A. A. (2002) Impact of isotropic superfinishing on contact and bending fatigue of carburized steel. *Proc. SAE International Off-Highway Congress*, Las Vegas, Paper No. 2002-01-1391.
16. Ishibashi, A., Ezoe, S. and Tanaka, S. (1984) *Mirror Finishing of Tooth Surfaces Using a Trial Gear Grinder with Cubic-Born-Nitride Wheel*. ASME Publication 84-DET-153, ASME, New York, NY.
17. Krantz, T. L., Alanou, M. P., Evans, H. P. and Snidle, R. W. (2001) Surface fatigue lives of case-carburized gears with an improved surface finish. *J. Tribol.* **123**, 709–716.
18. Breen, D. H. and Wene, E. M. (1979) Fatigue in Machines and Structures – Ground Vehicles. *Proc. American Society for Metals, Metals Park*, Ohio, 72.
19. Fuchs, H. O. (1986) *Mechanical Engineer's Handbook*. Wiley, New York.
20. Siebel, E. and Pfender, M. (1941) Weiterentwicklung der Festigkeitsberechnungen bei Wechselbeanspruchung. *Stahl und Eisen* **66/67**, 318–321.
21. Eichlseder, W. (2002) Fatigue analysis by local stress concept based on finite element results. *Comput. Struct.* **80**, 2109–2113.
22. Eichlseder, W. (2003) Lebensdauervorhersage auf Basis von Finite Elemente Ergebnissen (Fatigue Life prediction based on Finite Element Results). *Werkstofftech* **34**, 843–849.
23. Taylor, D. (2007) *The Theory of Critical Distances – A New Perspective in Fracture Mechanics*. Elsevier Science B.V., Amsterdam.
24. Pariente, I. F. and Guagliano, M. (2008) About the role of residual stresses and surface work hardening on fatigue ΔK_{th} of a nitrided and shot peened low-alloy steel. *Surface Coatings Technol.* **202**, 3072–3080.
25. Guagliano, M., Riva, E. and Guidetti, M. (2002) Contact fatigue failure analysis of shot-peened gears. *Eng. Fail. Anal.* **9**, 147–158.
26. Peyrac, C., Flavenot, J. F. and Convert, F. (2000) Combining case hardening and shot peening for gear steels: influence on residual stresses. *Mater. Sci. Forum* **347**, 435–440.

doi: 10.1111/j.1475-1305.2009.00685.x

27. Olmi, G. and Freddi, A. (2006) Shot peening technique for fatigue improvement of high strength steel gears. *Proc. 5th ICCSM*, Trgir/Split (Croatia). Paper number: 153.
28. Comandini, M., Olmi, G. and Freddi, A. (2007) Fatigue performance of shot-peened gears investigated by experimental and numerical methods. *Trans. Famena* **31–2**, 1–10.
29. Dixon, W. J. and Massey, F. J., Jr (1983) *Introduction to Statistical Analysis*. McGraw-Hill, New York.
30. Benedetti, M., Bortolamedi, T., Fontanari, V. and Frendo, F. (2004) Bending fatigue behaviour of differently shot peened Al 6082 T5 alloy. *Int. J. Fatigue* **26**, 889–897.
31. Leitner, H., Eichlseder, W., Godor, I., Waggermayer, M. and Hinteregger, C. (2005) Increased fatigue limit of gear wheels by a combination of case hardening and shot peening. *Proc. RELMAS 2005 (6th International Conference)*, St Petersburg (Russia).
32. Gänser, H.-P., Gódor, I., Leitner, H. and Eichlseder, W. (2006) Enhanced fatigue life by mechanical surface treatments – experiment and simulation. *Proc. 16th European Conference of Fracture*, Alexandroupolis (Greece).
33. Moore, M. G. and Evans, W. P. (1958) Correction for stress layers in X-ray diffraction residual stress analysis. *SAE Trans*. **66**, 340–345.
34. Bertini, L. and Fontanari, V. (1999) Fatigue behaviour of induction hardened notched components. *Int. J. Fatigue* **21**, 611–617.
35. Berger, P. D. and Maurer, R. E. (2002) *Experimental Design with applications in management, engineering and the sciences*. Duxbury Press, Belmont, CA.
36. Guagliano, M., Vergani, L., Bandini, M. and Gili, F. (1999) An approach to relate the shot-peening parameters to the induced residual stresses. *Proc. ICSP7*, Warsaw, 274–282.
37. Starker, P. and Macherauch, E. (1983) Shot peening and fatigue endurance. *Z. Werkstofftechnik* **14**, 109–115.
38. Leitner, H., Gänser, H.-P. and Eichlseder, W. (2007) Oberflächennachbehandlung durch Kugelstrahlen und Festwalzen-Mechanismen, Modellierung, Methoden. *Materialprüfung* **49**, 408–413.

doi: 10.1111/j.1475-1305.2009.00685.x